ISSN 0027-1349, Moscow University Physics Bulletin, 2024, Vol. 79, Suppl. 1, pp. S243–S251. © Allerton Press, Inc., 2024.

The Status of SATURNE

M. Cadeddu[1], F. Dordei[1], C. Giunti[2], A. P. Ivashkin[3], K. A. Kouzakov[4*], F. M. Lazarev[4], O. A. Moskalev[5], I. S. Stepantsov[4], A. I. Studenikin[4], I. I. Tkachev[3], V. N. Trofimov[6], M. A. Verkhovtsev[5,7], M. M. Vyalkov[5,7], A. A. Yukhimchuk[5], and E. F. Zagirdinova[4]

[1] *Istituto Nazionale di Fisica Nucleare (INFN), Sezione di Cagliari, Complesso Universitario di Monserrato S.P., Monserrato (Cagliari), 09042 Italy*

[2] *Istituto Nazionale di Fisica Nucleare (INFN), Sezione di Torino, Torino, 10125 Italy*

[3] *Institute for Nuclear Research, Russian Academy of Sciences, Moscow, 117312 Russia*

[4] *Faculty of Physics, Lomonosov Moscow State University, Moscow, 119991 Russia*

[5] *Russian Federal Nuclear Center—All-Russian Scientific Research Institute of Experimental Physics, Sarov, Nizhny Novgorod oblast, 607188 Russia*

[6] *Dzhelepov Laboratory of Nuclear Problems, Joint Institute for Nuclear Research, Dubna, Moscow oblast, 141980 Russia*

[7] *Branch of Lomonosov Moscow State University in Sarov, Sarov, Nizhny Novgorod oblast, Russia*

Received May 15, 2024; revised May 31, 2024; accepted June 1, 2024

Abstract—SATURNE is the Sarov tritium neutrino experiment that aims at the first observation of coherent elastic neutrino–atom scattering and the search for neutrino electromagnetic properties. A marked feature of the experiment is the use of a high-intensity tritium source of electron antineutrinos with a total tritium mass of at least 1 kg (10 MCi). Three detectors are being developed for the goals of the experiment. A 1-m^3 liquid He-4 detector operating at a temperature between 40 and 60 mK is designed both to register coherent elastic neutrino–atom scattering and to search for the neutrino magnetic moment at a level of $\mu_\nu \sim 10^{-13}\,\mu_{\rm B}$, which is about an order of magnitude better than the world-leading upper limits on the μ_ν value. A 4-kg Si crystal detector operating at a temperature in the range of 10–50 mK and a 14-kg SrI_2(Eu) scintillation detector operating at a temperature between −60 and −40 °C are purposed for testing the μ_ν value on the order of $\sim 10^{-12}\,\mu_{\rm B}$, which is competitive with or even better than the world-leading upper limits.

Keywords: SATURNE, coherent elastic neutrino–atom scattering, neutrino magnetic moment, tritium, liquid He-4 detector, Si crystal detector, SrI_2(Eu) scintillation detector

DOI: 10.3103/S0027134924701728

1. INTRODUCTION

The Sarov tritium neutrino experiment (SATURNE) is part of the scientific program of the National Center for Physics and Mathematics (NCPhM) [1] that was founded in Sarov in 2021. The experiment is under preparation, with the first taking of data expected for 2025 and the data collection expected to be completed by 2032.

SATURNE is motivated by fundamental problems in neutrino physics. Specifically, it will primarily search for neutrino electromagnetic interactions [2, 3] in elastic and ionizing neutrino–atom collisions. The experiment will employ a high-intensity tritium neutrino source, with an initial activity of at least 10 MCi and possibly up to 40 MCi. The tritium source will be used in combination with the He-4, Si, and SrI_2(Eu) targets in order to study the elastic and ionization channels of neutrino–atom collisions at unprecedentedly low energies.

The Si and SrI_2(Eu) detectors with record low-energy thresholds for such detector types will measure the ionization channel of neutrino–atom collisions. With the 1-year data from either detector, one may expect to achieve a sensitivity on the order of $\sim 10^{-12}\,\mu_{\rm B}$ at 90% C.L. to the neutrino magnetic moment μ_ν, which is the most studied theoretically

*E-mail: kouzakov@gmail.com

and actively searched experimentally among the neutrino electromagnetic properties.

The measurements with the liquid He-4 detector in a superfluid state are expected to provide the first observation of coherent elastic neutrino–atom scattering (CEνAS) [4, 5]. This will bring the experimental studies of coherent elastic neutrino–nucleus scattering (CEνNS) [6] to a qualitatively new level, namely when one will be able to explore the neutrino elastic scattering not only on a nucleus as a whole, but also on an atom as a whole. With the 5-year data using the liquid He-4 detector, it is also expected to achieve a record-high μ_ν-sensitivity of $\sim 10^{-13}\,\mu_{\rm B}$ at 90% C.L.

The paper is organized as follows. In Section 2, a brief overview of SATURNE is given. Section 3 outlines the physics that will be studied in SATURNE. Finally, a summary of this work and the outlook are presented in Section 4.

The units $\hbar = c = 1$ are used throughout unless otherwise specified.

2. OVERVIEW OF SATURNE

The key ingredients of SATURNE are (i) the high-intensity tritium source of electron antineutrinos, (ii) the liquid He-4 detector in a superfluid state, (iii) the cryogenic Si crystal detector, and (iv) the low-temperature SrI_2(Eu) scintillation detector. For conducting the SATURNE measurements, a low-background neutrino laboratory is being created at the NCPhM [1, 7]. For this purpose an existing shallow underground facility in Sarov is used. It is equipped with a service lift, waterproofed and meets the necessary requirements for working with a high-intensity tritium source. The facility has an overburden consisting of 4-m thick reinforced concrete, manufactured before the Atomic Age and in this regard pure in terms of uranium series elements, 5-m thick sand and a layer of soil, which is more than 0.5-m thick. The overburden is about 20–25 m of water equivalent, which is enough to sufficiently suppress the soft and hadronic components of cosmic radiation for acceptable background conditions.

2.1. Tritium Neutrino Source

Tritium is an unstable, radioactive isotope of hydrogen. It has a half-life of 12.3 years and decays via the β^- decay

$$^3{\rm H} \to {}^3{\rm He} + e^- + \bar{\nu}_e. \tag{1}$$

The energy spectrum of emitted electron antineutrinos lies in the range from 0 to 18.6 keV, with an average energy $\langle E_\nu \rangle = 12.9$ keV.

The principal design of a tritium neutrino source was worked out in [8] (see also [7]): it is a set of tubular elements, in which tritium is in a chemically bound state on titanium (TiT_2). Titanium powder in bulk form is placed in the tubular element. Then the titanium powder is thermally activated and saturated with tritium, after which the tubular element is sealed. This tubular element design will be classified as a "closed radionuclide source." According to the radiation safety regulations NRB-99/2009 "A closed radionuclide source is a radiation source, the design of which prevents the release of radionuclides contained in it into the environment under the conditions of use and wear for which it is designed." This implies that the design of the tubular element is made in such a way that it is possible to extract tritium from it only under special factory conditions.

The amount of tritium in each tubular element is not more than that permissible for its safe handling during transportation and operation, in accordance with current national and international standards. The mass of tritium in each tubular element is no more than 50 g (0.5 MCi). For a specific detecting system, the geometry of the tubular element must be selected according to the following conditions: (i) the efficiency of using neutrinos, (ii) ensuring the convenience of production and operation of the tubular element, and (iii) securing the safety of working with the tubular elements and the experimental apparatus as a whole.

2.2. Liquid He-4 Detector

Data collection using the liquid He-4 detector is planned for 2027–2032. Figure 1 shows the concept of the detector setup. The tritium neutrino source (TiT_2) is placed inside the hollow of the 1000-l cylinder tank filled with liquid He-4 in a superfluid state (He II). The dilution refrigerator keeps liquid He-4 at a temperature between 40 and 60 mK. An array of about 1000 transition edge sensors (TESs) [9] suspended in vacuum above the helium surface registers the evaporated He-4 atoms, which are induced by scattering of electron antineutrinos from the tritium β^- decay on atoms in the superfluid.[1] The signal from the TES bolometers is readout by a SQUID system. In such a way, the detector is expected to be sensitive to energy signals below 0.1 eV.

[1] The detection method using a superfluid He-4 target and a quantum evaporation channel is also being developed for light dark matter searches by HeRALD [10] and DELight [11].

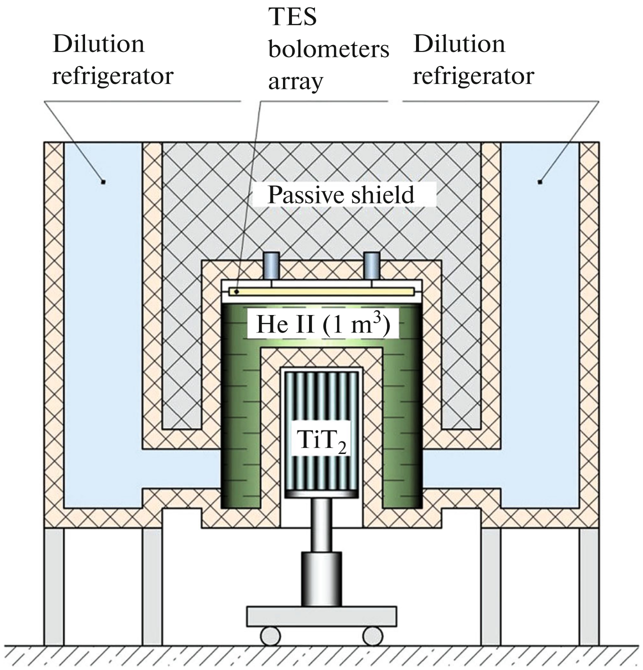

Fig. 1. A schematic drawing of the experimental setup with the liquid He-4 detector.

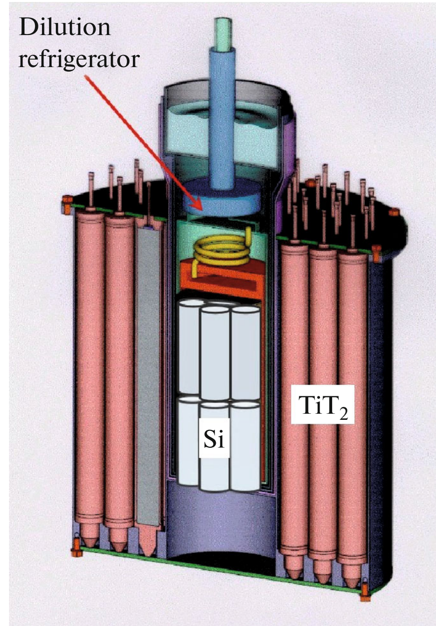

Fig. 2. A schematic drawing of the experimental setup with the Si detector.

2.3. Si Crystal Detector

Data collection using the Si detector is scheduled for 2026–2027. The detector is supposed to consist of fourteen 125-cm^3 Si crystal cylinders with a total mass of 4 kg (see Fig. 2), operating at a temperature between 10 and 50 mK. The low operating temperature is designed to take advantage of the Neganov–Trofimov–Luke effect [12 13], that is, when the conversion of ionization energy into heat is amplified by a (high) bias voltage. The heat is measured by microcalorimeters, such as TESs or semiconductor thermistors, which are mounted on each silicon cylinder. This may allow to achieve the energy threshold of the detector as low as about 10 eV or even 1 eV [14–16].

2.4. SrI$_2$(Eu) Scintillation Detector

Data collection using the SrI$_2$(Eu) detector is expected for 2025–2026. The scintillation detector is assumed to be an assembly of SrI$_2$(Eu) crystal elements with a total mass of 14 kg surrounding the tritium neutrino source as shown in Fig. 3. The elements, each having dimensions of $15 \times 15 \times 25$ mm^3 and a mass of 25 g, are combined into modules with four elements per module. The operating temperature of the detector is in the range from -60 to -40 °C. At such a temperature the thermal noise of silicon photomultipliers used for signal readout decreases sharply, thus making it possible to detect extremely low light signals, namely at the level of several photons only. This is expected to provide a record light collection and a detector threshold as low as 100 eV [17].

3. PHYSICS WITH SATURNE

In the Standard Model (SM), the neutrinos are massless particles coupled only to the Z^0 and $W^{\pm}$ gauge bosons. The established existence of non-zero neutrino masses opens up the possibility for neutrinos to have other properties that are beyond the SM. Of particular interest is the possibility for neutrinos to have electromagnetic characteristics, such as the electric charge (millicharge), charge radius, magnetic, electric and anapole moments. The discovery of neutrino electromagnetic properties will literally open a window to new physics [2].

So far, the most studied neutrino electromagnetic characteristic, both theoretically and experimentally,

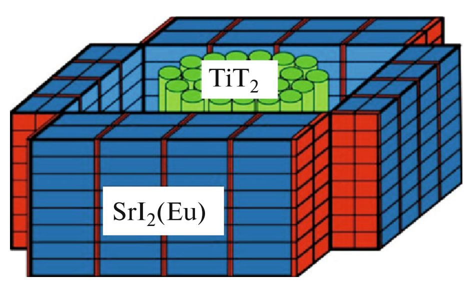

Fig. 3. The concept of the experimental scheme with the SrI$_2$(Eu) scintillation detector.

is the neutrino magnetic moment. A nonzero magnetic moment for neutrinos arises already in the minimal SM extension with the addition of the right-handed Dirac massive neutrinos. The predicted value is [18]

$$\mu_\nu = \frac{3\sqrt{\alpha}G_{\mathrm{F}}m_\nu}{8\sqrt{2}\pi^2} \approx 3.2\times10^{-19}\left(\frac{m_\nu}{1\,\mathrm{eV}}\right)\mu_{\mathrm{B}}, \quad (2)$$

where G_{F} is the Fermi constant, α is the fine-structure constant, m_ν is the neutrino mass, and μ_{B} is the Bohr magneton. Given the constraint on the neutrino mass $m_\nu < 0.8$ eV (at 90% C.L.) from the KATRIN experiment [19], the μ_ν value in Eq. (2) does not exceed $10^{-19}\,\mu_{\mathrm{B}}$ in the order of magnitude.

There are various theoretical scenarios beyond the minimally extended SM which predict much greater neutrino magnetic moment values than Eq. (2) (see [2] and references therein). Moreover, some of such theoretical predictions have been already ruled out by the world leading experimental constraints on the neutrino magnetic moment. Such constraints are obtained in laboratory experiments and astrophysics.

The strongest laboratory constrains are from the data on elastic neutrino-electron scattering, or atomic ionization (AI) by neutrinos. For solar neutrinos the most stringent upper bound is [20]

$$\mu_{\nu_\odot} < 6.3\times10^{-12}\,\mu_{\mathrm{B}}. \quad (3)$$

It was obtained from the analysis of the data of the XENONnT experiment at Gran Sasso, Italy [21]. The most stringent upper bound for reactor neutrinos is due to the GEMMA experiment at the Kalinin Nuclear Power Plant, Russia [22]:

$$\mu_{\bar\nu_e} < 2.9\times10^{-11}\,\mu_{\mathrm{B}}. \quad (4)$$

The most stringent astrophysical upper bounds on the μ_ν value were derived from the data on the luminosity of globular clusters [23–25]:

$$\mu_\nu < (1.2\text{-}2.6)\times10^{-12}\,\mu_{\mathrm{B}}. \quad (5)$$

Though these constraints are stronger than (3) and (4), they are indirect as opposed to the laboratory ones.

Thanks to the study of the ionization of atoms by tritium neutrinos, SATURNE has the potential to improve the laboratory limits to a level that makes them competitive or even better than the astrophysical limits. It has an even greater potential with studying the CEνAS channel. In such a case, the sensitivity to the μ_ν value can be almost an order of magnitude better than the astrophysical upper bounds (5).

3.1. AI Channel

The most sensitive and widely used method for the experimental investigation of the neutrino magnetic moment is provided by direct laboratory measurements of low-energy elastic scattering of neutrinos and antineutrinos with electrons in reactor, accelerator and solar experiments. Since in such measurements the initial electrons are typically bound in target atoms, the neutrino-electron collision results in AI.

Let us consider the process

$$\bar\nu_e + e^- \to \bar\nu_\ell + e^-, \quad (6)$$

where an electron antineutrino with energy E_ν elastically scatters off a free electron at rest in the laboratory frame. Due to neutrino electromagnetic interactions, the final antineutrino flavor ℓ can be different from the electron flavor. Experimentally, one usually measures the energy transfer T, or the energy deposited by the neutrino in the detector. In the free-electron case, the energy transfer amounts to the kinetic energy of the recoil electron, which is constrained from the energy-momentum conservation by

$$T \le \frac{2E_\nu^2}{2E_\nu + m_e}, \quad (7)$$

where m_e is the electron mass. For tritium $\bar\nu_e$'s the maximal energy is $E_{\nu,\max} = 18.6$ keV, so that $T \le$ 1.26 keV.

Since, in the ultrarelativistic limit, the neutrino magnetic moment interaction changes the neutrino helicity and the SM weak interaction conserves the neutrino helicity, the two contributions add incoherently in the differential cross section which can be written as

$$\frac{d\sigma^{\bar\nu_e e^-}}{dT} = \frac{d\sigma^{\bar\nu_e e^-}_{\mathrm{SM}}}{dT} + \frac{d\sigma^{\bar\nu_e e^-}_{\mu_\nu}}{dT}. \quad (8)$$

The SM cross section for neutrino scattering on a free electron is given by

$$\frac{d\sigma^{\bar\nu_e e^-}_{\mathrm{SM}}}{dT} = \frac{G_{\mathrm{F}}^2 m_e}{2\pi}\Big[(g_V+g_A)^2 + (g_V-g_A)^2\left(1-\frac{T}{E_\nu}\right)^2 + \left(g_A^2-g_V^2\right)\frac{m_eT}{E_\nu^2}\Big], \quad (9)$$

with the standard coupling constants

$$g_V = \frac{1}{2} + 2\sin^2\theta_W, \quad g_A = -\frac{1}{2},$$

where $\sin^2\theta_W = 0.23863(5)$ [26], calculated at vanishing momentum transfer in the $\overline{\mathrm{MS}}$ scheme.

The neutrino magnetic-moment contribution to the free-electron cross section is

$$\frac{d\sigma_{\mu_\nu}^{\bar{\nu}_e e^-}}{dT} = \frac{\pi\alpha^2}{m_e^2}\left(\frac{1}{T} - \frac{1}{E_\nu}\right)\left(\frac{\mu_{\bar{\nu}_e}}{\mu_{\rm B}}\right)^2, \qquad (10)$$

where $\mu_{\bar{\nu}_e}$ is the effective magnetic moment of the electron antineutrino [2].

The two contributions to the cross section, $d\sigma_{\rm SM}^{\bar{\nu}_e e^-}/dT$ and $d\sigma_{\mu_\nu}^{\bar{\nu}_e e^-}/dT$, depend on the experimentally observable energy transfer T in a qualitatively different way. One can see that small values of the neutrino magnetic moment can be probed by lowering the energy transfer threshold in experiment. Indeed, in the kinematical regime $T \ll E_\nu$ one has

$$\frac{d\sigma_{\rm SM}^{\bar{\nu}_e e^-}}{dT} \propto {\rm const}, \quad \frac{d\sigma_{\mu_\nu}^{\bar{\nu}_e e^-}}{dT} \propto \frac{1}{T},$$

and, hence, the lower the energy transfer the larger the μ_ν contribution relative to the SM one.

At low energy transfer values one can expect a modification of the free-electron formulas (9) and (10) due to the binding of electrons in atoms. It was demonstrated (see [27] and references therein) by means of analytical and numerical calculations that the atomic binding effects are adequately described by the so-called stepping approximation introduced in [28] from interpretation of numerical data. According to the stepping approach, the SM and μ_ν contributions to the AI differential cross section are calculated on the basis of

$$\frac{d\sigma_{\rm SM}^{\rm AI}}{dT} = \frac{d\sigma_{\rm SM}^{\bar{\nu}_e e^-}}{dT}\sum_j n_j\theta(T - E_j), \qquad (11)$$

$$\frac{d\sigma_{\mu_\nu}^{\rm AI}}{dT} = \frac{d\sigma_{\mu_\nu}^{\bar{\nu}_e e^-}}{dT}\sum_j n_j\theta(T - E_j), \qquad (12)$$

where the j sum runs over all occupied atomic (sub)levels, with n_j and E_j being their occupations and binding energies. The typical dependencies of the SM and μ_ν differential cross sections for AI on the energy transfer T are illustrated in Fig. 4, which presents the numerical results based on the stepping approximation for ionization of the Si atom by an electron antineutrino from the tritium β^- decay.

Tables 1 and 2 show the projected number of the SM $\bar{\nu}_e e^-$-scattering events $N_{\rm SM}^{\bar{\nu}_e e^-}$ and the μ_ν-sensitivity after one year of data collection in SATURNE using a tritium neutrino source with an activity of 10 MCi and respectively the Si and SrI_2(Eu) detectors. The projected sensitivity to the neutrino magnetic moment is presented depending on the detector's energy threshold $E_{\rm th}$ that can be achieved (see Section 2). It is estimated in terms of the least-square function $\Delta\chi^2 = \chi^2 - \chi^2_{\rm min}$, with

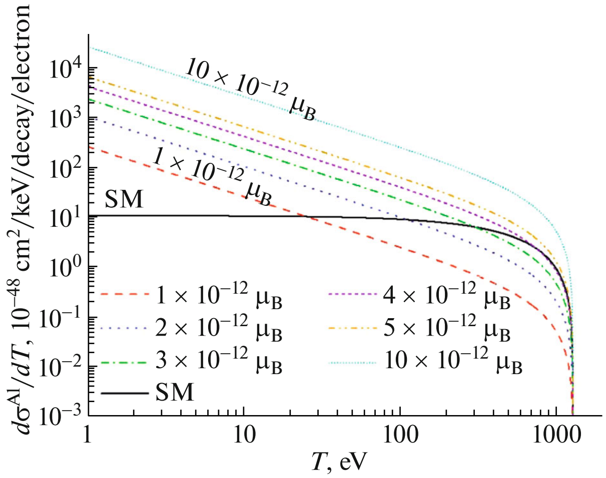

Fig. 4. The SM and μ_ν contributions to the AI differential cross section in the case of the tritium neutrino source and Si atomic target.

$$\chi^2(\mu_{\bar{\nu}_e}) = \left(\frac{N_{\rm SM}^{\bar{\nu}_e e^-} - N^{\bar{\nu}_e e^-}(\mu_{\bar{\nu}_e})}{\sqrt{N_{\rm SM}^{\bar{\nu}_e e^-}}}\right)^2, \qquad (13)$$

where $N^{\bar{\nu}_e e^-}(\mu_{\bar{\nu}_e})$ is the number of the $\bar{\nu}_e e^-$-scattering events for a given value of $\mu_{\bar{\nu}_e}$.

3.2. CEνAS Channel

The process of coherent elastic neutrino-atom scattering was predicted many years ago by Gaponov and Tikhonov [4], using the framework of the $V - A$ theory of weak interaction. They showed that at neutrino energies $E_\nu \lesssim 10$ keV a region of coherent optical neutrino phenomena exists where the neutrino elastic scattering by an atom as a whole dominates.

Although it is almost half a century since CEνAS was predicted, it is still to be observed in experiment. The difficulty of experimental investigation of CEνAS is largely related to the necessity of measuring very small values of transferred energy T, satisfying the coherence condition $qR_a \lesssim 1$, where $q = \sqrt{2m_aT}$ is

Table 1. The expected number of SM events $N_{\rm SM}^{\bar{\nu}_e e^-}$ and sensitivity to $\mu_{\bar{\nu}_e}$ after one year of collecting the $\bar{\nu}_e e^-$-scattering data with the Si detector in the case of 10-MCi tritium activity

$E_{\rm th}$, eV	$N_{\rm SM}^{\bar{\nu}_e e^-}$	Sensitivity to $\mu_{\bar{\nu}_e}$ at 90% C.L.
1	10.8	$1.6\times10^{-12}\,\mu_{\rm B}$
10	10.8	$1.9\times10^{-12}\,\mu_{\rm B}$

Table 2. The same as in Table 1, but in the case of the $SrI_2(Eu)$ scintillation detector

$E_{\rm th}$, eV	$N_{\rm SM}^{\bar{\nu}_e e^-}$	Sensitivity to $\mu_{\bar{\nu}_e}$ at 90% C.L.
100	24.3	$2.0\times10^{-12}\,\mu_{\rm B}$
200	22.2	$2.3\times10^{-12}\,\mu_{\rm B}$
300	19.5	$2.7\times10^{-12}\,\mu_{\rm B}$
400	16.6	$3.1\times10^{-12}\,\mu_{\rm B}$

Table 3. The expected number of SM and μ_ν events, $N_{\rm SM}^{{\rm CE}\nu{\rm AS}}$ and $N_{\mu_\nu}^{{\rm CE}\nu{\rm AS}}$, in the liquid He detector after five years of collecting data

Tritium activity	$N_{\rm SM}^{{\rm CE}\nu{\rm AS}}$	$N_{\mu_\nu}^{{\rm CE}\nu{\rm AS}}$ for $\mu_{\bar{\nu}_e}$	
		$3\times10^{-13}\,\mu_{\rm B}$	$10^{-12}\,\mu_{\rm B}$
10 MCi	58.9	7.8	90.1
40 MCi	295.2	27.1	298.8

the momentum transfer value, R_a is the atomic radius and m_a is the atomic mass. Already for light atoms ($R_a \sim 0.1$ nm and $m_a \sim$ few GeV) such T values appear not to exceed several hundreds of meV (see below). In addition, an intense neutrino source with $E_\nu \lesssim 10$ keV is needed. The latter requirement, in particular, hinders the observation of CEνAS in the CEνNS experiments [6], which employ reactor and accelerator sources with typical (anti)neutrino energies of the order of a few MeV and tens of MeV, respectively.

In the case of the tritium neutrino source, the atomic recoil energy, which amounts to the energy transfer T in CEνAS, is restricted to

$$T \le T_{\rm max} = \frac{2E_{\nu,\rm max}^2}{2E_{\nu,\rm max} + m_a} \simeq \frac{743}{A}\ {\rm meV}, \qquad (14)$$

where A is the atomic mass number. SATURNE will study the process of elastic scattering of a tritium $\bar{\nu}_e$ on a He-4 atom ($A = 4$),

$$\bar{\nu}_e + {\rm He} \to {\rm He} + \bar{\nu}_\ell, \qquad (15)$$

where the final flavor ℓ can differ from the electron flavor if neutrino electromagnetic interactions are present.

The differential cross section for the process (15) can be presented as

$$\frac{d\sigma^{{\rm CE}\nu{\rm AS}}}{dT} = \frac{d\sigma_{\rm SM}^{{\rm CE}\nu{\rm AS}}}{dT} + \frac{d\sigma_{\mu_\nu}^{{\rm CE}\nu{\rm AS}}}{dT}. \qquad (16)$$

The contribution from the SM weak interaction has the form

$$\frac{d\sigma_{\rm SM}^{{\rm CE}\nu{\rm AS}}}{dT} = \frac{G_{\rm F}^2 m_{\rm He}}{\pi} C_V^2 \left(1 - \frac{m_{\rm He} T}{2E_\nu^2}\right), \qquad (17)$$

with

$$C_V = Z\left(\frac{1}{2} - 2\sin^2\theta_W\right) - \frac{1}{2}N + Z\left(\frac{1}{2} + 2\sin^2\theta_W\right) F_{\rm el}(q^2),$$

where $Z = N = 2$ is the proton (Z) and neutron (N) number in He-4, $m_{\rm He} = 3.728$ GeV is the He-4 atomic mass, $q^2 = 2m_{\rm He}T$, and $F_{\rm el}(q^2)$ is the Fourier-transform of the atomic electron density normalized to unity, or the atomic form factor.

The contribution from the neutrino magnetic moment is

$$\frac{d\sigma_{\mu_\nu}^{{\rm CE}\nu{\rm AS}}}{dT} = \frac{\pi\alpha^2 Z^2}{m_e^2}\left(\frac{\mu_{\bar{\nu}_e}}{\mu_{\rm B}}\right)^2 \left(\frac{1}{T} - \frac{1}{E_\nu} + \frac{T}{4E_\nu^2}\right) \times \left[1 - F_{\rm el}(q^2)\right]^2. \qquad (18)$$

Figure 5 shows the differential cross section (16) averaged over the tritium neutrino energy spectrum. Such a cross section, up to a constant factor, gives the He-4 atomic recoil spectrum in the CEνAS process with a tritium neutrino source. The SM prediction exhibits a marked feature at $T \simeq 9$ meV, namely a complete screening of the weak nuclear charge by the weak electron charge in the He-4 atom [5]. It can be seen that the neutrino magnetic moment contribution can lead to a substantial deviation from the SM prediction. As demonstrated in [29], in the He-4 case the deviation turns out to be much more pronounced than in the cases of lighter atomic targets, that is, such as the H, D, and He-3 atoms.

The projected sensitivity of the liquid He-4 detector to the neutrino magnetic moment is shown in Fig. 6. It is calculated in terms of the least-square function $\Delta\chi^2 = \chi^2 - \chi^2_{\rm min}$, with

$$\chi^2(\mu_{\bar{\nu}_e}) = \left(\frac{N_{\rm SM}^{{\rm CE}\nu{\rm AS}} - N^{{\rm CE}\nu{\rm AS}}(\mu_{\bar{\nu}_e})}{\sqrt{N_{\rm SM}^{{\rm CE}\nu{\rm AS}}}}\right)^2, \qquad (19)$$

where $N_{\rm SM}^{{\rm CE}\nu{\rm AS}}$ and $N^{{\rm CE}\nu{\rm AS}}(\mu_{\bar{\nu}_e})$ are the expected average numbers of events within SM ($\mu_{\bar{\nu}_e} = 0$) and for a given $\mu_{\bar{\nu}_e}$ value, respectively. The $N_{\rm SM}^{{\rm CE}\nu{\rm AS}}$ and $N_{\mu_\nu}^{{\rm CE}\nu{\rm AS}} = N^{{\rm CE}\nu{\rm AS}}(\mu_{\bar{\nu}_e}) - N_{\rm SM}^{{\rm CE}\nu{\rm AS}}$ values after five years of collecting data for minimal and maximal anticipated initial activity of the tritium source in SATURNE are presented in Table 3. As follows from Fig. 6, SATURNE can achieve the sensitivity to

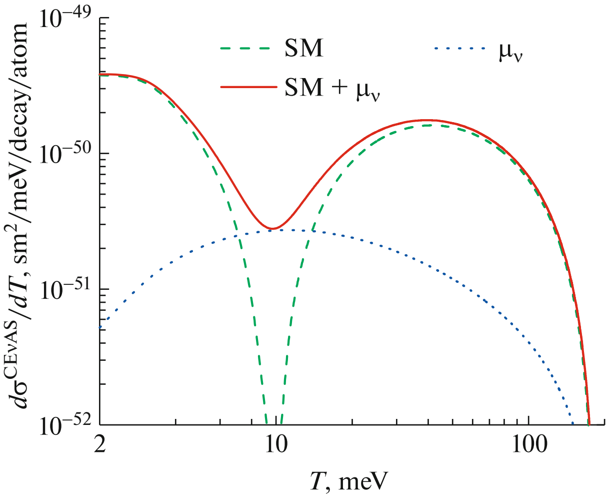

Fig. 5. The CEνAS differential cross section (solid curve) in the case of the tritium neutrino source and He-4 atomic target for $\mu_{\bar{\nu}_e} = 3 \times 10^{-13}\ \mu_{\rm B}$. Dashed and dotted curves represent the SM and μ_ν contributions, respectively.

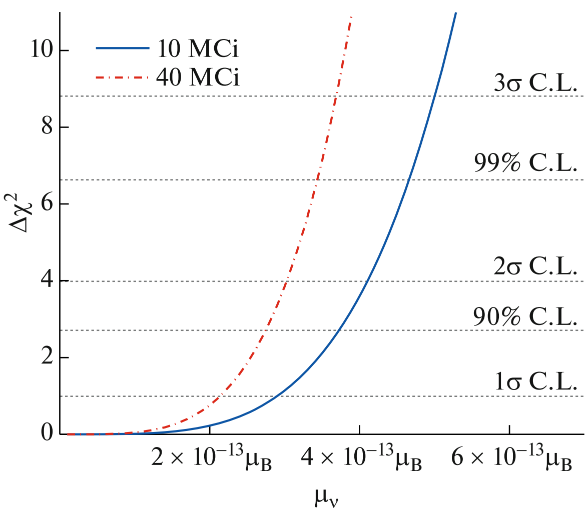

Fig. 6. The projected sensitivity to the $\mu_{\bar{\nu}_e}$ value after five years of data collection with the liquid He-4 detector in SATURNE. The solid curve corresponds to an initial tritium activity of 10 MCi, and the dash-dotted curve to that of 40 MCi.

the $\mu_{\bar{\nu}_e}$ value as high as about $(2.5-3.5) \times 10^{-13}\ \mu_{\rm B}$ at 90% C.L., depending on the initial activity of the tritium source: the higher the intensity, the better the sensitivity.

4. SUMMARY AND OUTLOOK

The tritium neutrino experiment, SATURNE, is under preparation at the NCPhM in Sarov. Its major goal is the first observation of coherent elastic neutrino-atom scattering, in order to test SM neutrino interactions at unprecedentedly low energies and to search for new physics, in particular, such as the neutrino magnetic moment. For these purposes, a low-background neutrino laboratory is being created and a high-intensity tritium neutrino source is being prepared with a tritium mass of at least 1 kg (10 MCi), and possibly up to 4 kg (40 MCi).

A 1000-l superfluid helium-4 detector is being developed for the first observation of coherent elastic neutrino-atom scattering. After five years of collecting data, by 2032, it is expected to achieve the neutrino magnetic moment sensitivity which is by an order of magnitude better than the current world leading constraints. Such a detector will have a rich potential to be also used for light dark matter searches with a superfluid helium target [10, 11].

A 14-kg SrI_2(Eu) scintillation detector and a 4-kg Si crystal detector are being developed for studying atomic ionization by tritium neutrinos. After one year of data-taking, by 2026 and 2027, respectively, they are expected to achieve the neutrino magnetic moment sensitivity that is competitive with or even better than the current world leading constraints. Both detectors will have record low-energy thresholds for their respective types of detection systems and, upon completion of the experiment, can be used in other areas of fundamental and applied physics. For example, the SrI_2(Eu) scintillation detector can be used in CEνNS measurements with reactor neutrinos, in the search for neutrinoless double beta decay, to identify isotopes in applied research and the nuclear industry. The Si crystal detector can also be used in the CEνNS measurements with reactor neutrinos and in the dark matter searches with cryogenic semiconductor targets [30, 31].

ACKNOWLEDGMENTS

We wish to acknowledge useful discussions with A. Pankratov, A. Gordeeva, A. Mel'nikov, and V. Eremin.

FUNDING

This work was supported by the Russian Science Foundation (project no. 24-12-00084). O.A. Moskalev is grateful for access to the scientific infrastructure provided within the framework of the scientific program of the National Center for Physics and Mathematics (section no. 8 "Physics of hydrogen isotopes," project "Fundamental studies in the field of neutrino physics and neutron-rich nuclei using isotopes of hydrogen and helium").

CONFLICT OF INTEREST

The authors declare that they have no conflicts of interest.

REFERENCES

1. A. A. Yukhimchuk, A. N. Golubkov, I. P. Maximkin, I. L. Malkov, O. A. Moskalev, R. K. Musyaev, A. A. Seleznev, L. V. Grigorenko, V. N. Trofimov, A. S. Fomichev, A. V. Golubeva, V. N. Verbetsky, K. A. Kouzakov, S. V. Mitrokhin, A. I. Studenikhin, A. P. Ivashkin, and I. I. Tkachev, Fizmat **1**, 5 (2023). https://doi.org/10.56304/S2949609823010057
2. C. Giunti and A. Studenikin, Rev. Mod. Phys. **87**, 531 (2015). https://doi.org/10.1103/RevModPhys.87.531
3. A. I. Studenikin and K. A. Kouzakov, Mosc. Univ. Phys. Bull. **75**, 379 (2020). https://doi.org/10.3103/S0027134920050215
4. Y. V. Gaponov and V. N. Tikhonov, Sov. J. Nucl. Phys. **26**, 314 (1977).
5. M. Cadeddu, F. Dordei, C. Giunti, K. A. Kouzakov, E. Picciau, and A. I. Studenikin, Phys. Rev. D **100**, 73014 (2019). https://doi.org/10.1103/PhysRevD.100.073014
6. V. Pandey, Prog. Part. Nucl. Phys. **134**, 104078 (2024). https://doi.org/10.1016/j.ppnp.2023.104078
7. O. Moskalev, A. Yukhimchuk, I. Maksimkin, et al., Mosc. Univ. Phys. Bull. **79** (7) (2024).
8. A. A. Yukhimchuk, Yu. I. Vinogradov, A. N. Golubkov, S. K. Grishechkin, R. I. Il'kaev, A. V. Kuryakin, B. L. Lebedev, V. N. Lobanov, V. N. Mikhailov, D. P. Tumkin, and L. N. Bogdanova, Fusion Sci. Technol. **48**, 731 (2005). https://doi.org/10.13182/FST05-A1026
9. V. Yu. Safonova, A. V. Gordeeva, A. V. Blagodatkin, D. A. Pimanov, A. A. Yablokov, O. L. Ermolaeva, and A. L. Pankratov, Materials **17**, 222 (2024). https://doi.org/10.3390/ma17010222
10. S. A. Hertel, A. Biekert, J. Lin, V. Velan, and D. N. McKinsey, Phys. Rev. D **100**, 92007 (2019). https://doi.org/10.1103/PhysRevD.100.092007
11. B. von Krosigk, K. Eitel, Ch. Enss, T. Ferber, L. Gastaldo, F. Kahlhoefer, S. Kempf, M. Klute, S. Lindemann, M. Schumann, F. Toschi, and K. Valerius, SciPost Phys. Proc. **12**, 16 (2023). https://doi.org/10.21468/SciPostPhysProc.12.016
12. B. Neganov and V. Trofimov, SU Inventor's Certificate No. 1037771, Otkrytia Izobreteniya (1985).
13. P. N. Luke, J. Appl. Phys. **64**, 6858 (1988). https://doi.org/10.1063/1.341976
14. V. N. Trofimov, B. S. Neganov, and A. A. Yukhimchuk, Phys. At. Nucl. **61**, 1271 (1998).
15. B. S. Neganov, V. N. Trofimov, A. A. Yukhimchuk, and L. N. Bogdanova, Phys. At. Nucl. **64**, 261 (2001). https://doi.org/10.1134/1.1349448
16. B. S. Neganov, V. N. Trofimov, A. A. Yukhimchuk, L. N. Bogdanova, A. G. Beda, and A. S. Starostin, Phys. At. Nucl. **64**, 1948 (2001). https://doi.org/10.1134/1.1423744
17. D. N. Abdurashitov, A. P. Vlasenko, A. P. Ivashkin, S. V. Silaeva, and V. V. Sinev, Phys. At. Nucl. **85**, 701 (2022). https://doi.org/10.1134/S1063778823010015
18. K. Fujikawa and R. E. Shrock, Phys. Rev. Lett. **45**, 963 (1980). https://doi.org/10.1103/PhysRevLett.45.963
19. M. Aker, A. Beglarian, J. Behrens, A. Berlev, U. Besserer, B. Bieringer, F. Block, S. Bobien, M. Böttcher, B. Bornschein, et al. (KATRIN Collab.), Nat. Phys. **18**, 160 (2022). https://doi.org/10.1038/s41567-021-01463-1
20. A. Khan, Phys. Lett. B **837**, 137650 (2023). https://doi.org/10.1016/j.physletb.2022.137650
21. E. Aprile, K. Abe, F. Agostini, S. Ahmed Maouloud, L. Althueser, B. Andrieu, E. Angelino, J. R. Angevaare, V. C. Antochi, D. A. Martin, F. Arneodo, L. Baudis, A. L. Baxter, L. Bellagamba, R. Biondi, A. Bismark, A. Brown, S. Bruenner, G. Bruno, R. Budnik, et al. (XENON Collab.), Phys. Rev. Lett. **129**, 161805 (2022). https://doi.org/10.1103/PhysRevLett.129.161805
22. A. G. Beda, V. B. Brudanin, V. G. Egorov, D. V. Medvedev, V. S. Pogosov, M. V. Shirchenko, and A. S. Starostin, Adv. High Energy Phys. **2012**, 350150 (2012). https://doi.org/10.1155/2012/350150
23. N. Viaux, M. Catelan, P. B. Stetson, G. G. Raffelt, J. Redondo, A. A. R. Valcarce, and A. Weiss, Astron. Astrophys. **558**, A12 (2013). https://doi.org/10.1051/0004-6361/201322004.
24. S. Arceo-Díaz, K.-P. Schröder, K. Zuber, and D. Jack, Astropart. Phys. **70**, 1 (2015). https://doi.org/10.1016/j.astropartphys.2015.03.006
25. F. Capozzi and G. Raffelt, Phys. Rev. D **102**, 83007 (2020). https://doi.org/10.1103/PhysRevD.102.083007
26. R. L. Workman, V. D. Burkert, V. Crede, E. Klempt, U. Thoma, L. Tiator, K. Agashe, G. Aielli, B. C. Allanach, C. Amsler, M. Antonelli, E. C. Aschenauer, D. M. Asner, H. Baer, S. Banerjee, R. M. Barnett, L. Baudis, C. W. Bauer, J. J. Beatty, V. I. Belousov, J. Beringer, A. Bettini, et al. (Particle Data Group), Prog. Theor. Exp. Phys. **2022**, 083C01 (2022). https://doi.org/10.1093/ptep/ptac097
27. K. A. Kouzakov and A. I. Studenikin, Adv. High Energy Phys. **2014**, 569409 (2014). https://doi.org/10.1155/2014/569409
28. V. I. Kopeikin, L. A. Mikaelyan, V. V. Sinev, and S. A. Fayans, Phys. At. Nucl. **60**, 1859 (1997).
29. G. V. Donchenko, K. A. Kouzakov, and A. I. Studenikin, JETP Lett. **117**, 879 (2023). https://doi.org/10.1134/S0021364023600982

30. M. F. Albakry, I. Alkhatib, D. W. P. Amaral, T. Aralis, T. Aramaki, I. J. Arnquist, I. Ataee Langroudy, E. Azadbakht, S. Banik, C. Bathurst, D. A. Bauer, R. Bhattacharyya, P. L. Brink, R. Bunker, B. Cabrera, R. Calkins, R. A. Cameron, C. Cartaro, D. G. Cerdeño, Y.-Y. Chang, et al., Phys. Rev. D **105**, 112006 (2022).
https://doi.org/10.1103/PhysRevD.105.112006

31. E. Armengaud, Q. Arnaud, C. Augier, A. Benoît, L. Bergé, J. Billard, A. Broniatowski, P. Camus, A. Cazes, M. Chapellier, F. Charlieux, M. De Jésus, L. Dumoulin, K. Eitel, J.-B. Filippini, et al. (EDELWEISS Collab.), Phys. Rev. D **106**, 62004 (2022).
https://doi.org/10.1103/PhysRevD.106.062004